



ISSN: 2230-9926

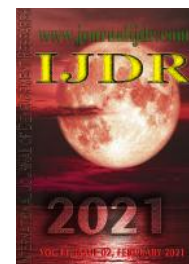
Available online at <http://www.journalijdr.com>

IJDR

International Journal of Development Research

Vol. 11, Issue, 02, pp. 44216-44221, February, 2021

<https://doi.org/10.37118/ijdr.21144.02.2021>



RESEARCH ARTICLE

OPEN ACCESS

SYNTHESIS OF CHROMOGEN FILMS OF METAL OXIDES USED AS SEMICONDUCTORS IN ADVANCED OXIDATIVE PROCESSES

Luana Góes Soares da Silva* and Annelise Kopp Alves

Department Engineering Materials, Universidade Federal do Rio Grande do Sul

ARTICLE INFO

Article History:

Received 07th November, 2020
Received in revised form
24th December, 2020
Accepted 18th January, 2021
Published online 24th February, 2021

Key Words:

Chromogen Films,
Heterogeneous Photocatalysis,
Spin-coating, TiO₂

*Corresponding author:

Luana Góes Soares da Silva

ABSTRACT

TiO₂ is a semiconductor used commercially as a material to impart opacity to paints, cosmetics, plastics and papers. It has three allotropes, anatase, brookite and rutile. Doping of TiO₂ with metals is an option to increase its ability to absorb radiation in the visible spectrum. In this work, metal oxide chromogen films were synthesized by *spin-coating*. For this, first TiO₂ and TiO₂ fibers containing H₂WO₄ or Na₂WO₄·2H₂O were obtained by *electrospinning*. These fibers were treated at temperatures ranging between 650 °C and 800 °C. The samples were characterized by X-ray diffraction (XRD) in order to determine the phases formed, the morphology was observed through a scanning electron microscope (SEM), the chromogenism of the films was observed through colorimetric tests, performed with the aid of a Konica-Minolta spectrophotometer. And the photoactivity was determined by means of degradation tests of 125 mL of a 20 ppm solution of the orange methyl dye, using the chromogenic films as semiconductors in the presence of UV-vis radiation. The results showed that the chromogenic films containing TiO₂/Na₂WO₄·2H₂O present greater effectiveness in the degradation of the orange methyl dye, due to the increase in the calcination temperature, which caused a disorder in the electronic structure of the samples, while decreasing the band gap of these, favoring their optical and photocatalytic properties. The increase in thermal excitation promoted the electrons from the valence band to the conduction band, intensifying the light absorption and degradation capacity of the films.

Copyright © 2020, Luana Góes Soares da Silva and Annelise Kopp Alves. This is an open access article distributed under the Creative Commons Attribution License, which permits unrestricted use, distribution, and reproduction in any medium, provided the original work is properly cited.

Citation: Luana Góes Soares da Silva and Annelise Kopp Alves. "Synthesis of Chromogen Films of Metal Oxides Used as Semiconductors in Advanced Oxidative Processes", *International Journal of Development Research*, 11, (01), 44216-44221.

INTRODUCTION

The glasses are a familiar group of ceramic materials applied in the manufacture of containers, windows, lenses, fiberglass, among others. Generally, they consist of non-crystalline silicates which also contain other oxides, some examples include CaO, Na₂O, K₂O, Al₂O₃, WO₃ and TiO₂, which influence their properties. The main characteristics of glassy materials involve their optical transparency and the ease with which they can be produced (Callister, 2002). Glass is produced by heating raw materials to a high temperature, above which melting occurs. Commercial glasses are generally of the silica, soda and lime type. In our study, we used (films) in suspension or immobilized as photocatalysts, due to the possibility of recovering the photocatalyst, decreasing the operational costs of the process, enabling its recovery and subsequent reuse (Oshani, 2014).

Advanced Oxidative Processes can be classified into homogeneous and heterogeneous systems. Its base of action resides in the generation of hydroxyl radicals (•OH), with high oxidizing power, which allow the complete mineralization of several organic compounds (Fioreze, 2014). Its mechanism of action occurs by adding to the double bond or by removing the hydrogen atom in oxidizing organic aliphatic molecules such as: ozone and hydrogen peroxide; associated with ultraviolet (UV) or visible (Vis) radiation and catalysts or semiconductors. The interaction of these reactions results in the formation of organic radicals, which react with oxygen, leading to degradation reactions (Fioreze, 2014). Within this context, this work evaluated how the eyes perceive the chromogenic variations that occur in TiO₂ and TiO₂ films containing tungsten precursors (H₂WO₄ and Na₂WO₄·2H₂O) as well as their photocatalytic performance, when irradiated by UVA-vis light.

METHODOLOGY

Electrospinning: To obtain fibers using *electrospinning*, the preparation of three precursor solutions (Figure 1) was required. The TiO₂ precursor solution was obtained by mixing 2.5 mL of titanium propoxide (Sigma-Aldrich), 2.0 mL of glacial acetic acid (Sigma-Aldrich) and 5.0 mL of an alcoholic solution containing 10 %wt of polyvinylpyrrolidone (PVP, 1,300,000 g/mol, Sigma-Aldrich). The TiO₂/WO₃ precursor solution was prepared by mixing the aforementioned reagents plus 0.10 g tungstic acid (H₂WO₄, Sigma-Aldrich) and 1 mL hydrogen peroxide (H₂O₂). This mixture was magnetic stirred at room temperature for 1 hour. Similar procedure was made to obtain the TiO₂/Na₂WO₄·2H₂O precursor solution but it was added 0.10 g of sodium tungstate dihydrate (TiO₂/Na₂WO₄·2H₂O) and 1 mL of hydrogen peroxide (H₂O₂). Then, a connection between a plastic syringe, loaded with 5 mL of the precursor solution, was set to a stainless steel hypodermic needle connected to the high voltage source. The distance between the needle tip and the cylindrical collector was 12 cm. It was applied a voltage of 13.5 kV in the system. An infusion pump controlled the flow of precursor solution (1.8 mL/h). The cylindrical collector was covered with an aluminum foil to easily collect the produced fibers every 30 minutes during 4 hours. The fibers were subjected to heat treatment in an electric furnace (SANCHIS) at temperatures of 650 °C, 700 °C, 750 °C or 800 °C (Figure 2), using a heating rate of 1.4 °C/h and a 1h dwell time at the highest temperature.

Spin-Coating: A solution containing 8 mL of ethanol (Zeppelin), 0.8 mL of acetylacetone (Sigma-Aldrich), 0.1 mL of Triton X-100 (Synth), 0.4 g of polyvinyl butyral (PVB, Sigma-Aldrich) and 0.50 g of heat-treated fibers were made. Firstly, the fibers were ultrasonically dispersed in acetylacetone, then the other chemicals were added and magnetic stirred for 5 minutes. Thin films were obtained using 5 drops of one of the said solutions over a glass plate (30 mm x 15 mm) pre-coated with FTO (*Fluorine-Doped Tin Oxide, Xop Glass*), using a TC 100 spin coater at 800 rpm for 30s.

RESULTS AND DISCUSSION

The distribution of the fibers in the films is shown in Figure 3. The TiO₂ fibers are randomly oriented with diameters between 0.20 and 0.35 μm. The microstructure of film TiO₂/WO₃ exhibited fibers with uneven nanorods aspect with some clusters of WO₃, and an average diameter between 28.5 and 60 μm. The agglomerates found in TiO₂/Na₂WO₄·2H₂O fibers can be attributed to the presence of WO₃. These samples have elongated fibers with irregular surfaces with diameters between 38 and 117.2 μm. There was a significant difference regarding the morphology of the heat-treated films, possible due to the sintering temperature itself, which promotes the removal of organic compounds and PVP, and the presence of sodium tungstate dihydrate and tungsten trioxide in doped samples.

Characterization: A scanning electron microscope (SEM, JEOL JSM 6060) was used to observe the morphology of the obtained materials. The average diameter of the fibers was estimated with the aid of the UTHSCSA *Image Tool* program. A X-ray diffraction equipment (Pan Analytical X'PERT, CuK_α, 40 kV - 40 mA) and the X'Pert *High Score* software were used to collect and analyze the XRD data, respectively.

The colorimetric analyzes were made using a spectrophotometer (Konica-Minolta CM-2600d) with integrating sphere and an UV filter. Samples were sandwiched between two glass plates using a pattern as a colorant. As illuminant it was used D65 which corresponds to the spectral range of daylight. The reflected color measurement simulates an observer at 10°. The photocatalytic activity of the fibers in comparison to the catalyst TiO₂-P25 (Evonik) was evaluated following the procedures used by Soares 2018, using a Cary Agilent 7000 spectrophotometer with the UMA accessory.

CIELa*b* System: The chromogenism, that is, the color change in the films was determined by associating the CIELa*b* system with the human capacity to see and differentiate the values of E*ab (DIN 6174, 1979) [Silva, 2007]. The i7 software that comes with the spectrophotometer, records and analyzes the colorimetric information through the CIELa*b* system. In this system, the color is determined according to the positive or negative values of the coordinates a* (red and green) and b* (yellow and blue). L* defines luminescence ranging from 0 to 100%.

The films without heat-treatment appear to be amorphous. In the TiO₂ film, up to 700 °C only anatase was identified by XRD (Figure 4a). From 750 °C up, the presence of rutile and anatase was detected probably as a result of a phase transformation due to the increase of the heat treatment temperature (Feltrin, 2013). The TiO₂/WO₃ films (Figure 4b), on the other hand, exhibited characteristic peaks at 2θ = 23.34, 23.64, 24.80, 32.85, 34.84°, among others, indicating the presence of tungsten components and its monoclinic phase. It was also possible to identify the presence of anatase, brookite and rutile (Feltrin, 2013). The TiO₂/Na₂WO₄·2H₂O films (Figure 4c) presented the anatase, brookite and rutile, tetragonal and triclinic phases of WO₄, and the presence of the Na(OH) group resulting from the use of Na₂WO₄·2H₂O.

The results of the chromogens tests performed on the films of the standard P25, TiO₂, TiO₂/WO₃ and TiO₂/Na₂WO₄·2H₂O are shown in Table 1. The records for each sample were obtained based on the CIE-La*b* system and, the measurement range covered the entire visible spectrum (400 to 700 nm). Table 1 also shows the luminescence values (% L), that is, the amount of light that is perceived in a given color. If the luminescence (% L) is close to 0% it represents the total absence of reflected light (black) and if it is close to 100% it represents the total reflection of light (white) (Soares, 2018). And the L* values, which inform about the differences between the shades in lighter or darker. Positive (+) values for L* indicate the lightest color and negative (-) values for L* indicate the darkest color. In colorimetric analyzes, the maximum absorbance occurs in the complementary staining region. The results were obtained with the help of the *i7 software* that accompanies the equipment and records various information for each analysis, the most useful for defining the region of maximum absorbance, those of the CIELa*b* system. The TiO₂ films had maximum light absorbance in the region of the dark blue color influenced by the positive values of a* (red color) and negative values of b* (blue color). This result was already expected, as the color of the TiO₂ solution is light yellow (Figure 1a), which is the complementary color to blue. The TiO₂/WO₃ films, on the other hand, had maximum light absorbance in the light blue color region, influenced by the negative values of a* (green color) and negative values of b* (blue color).



Figure 1. Color photograph of the precursor solutions for the synthesis of fibers by electrospinning, (a) TiO_2 , (b) TiO_2/WO_3 and (c) $\text{TiO}_2/\text{Na}_2\text{WO}_4 \cdot 2\text{H}_2\text{O}$, respectively



FIGURE 2. Photographic image of fibers obtained by electrospinning, (a) Without heat treatment, (b) TiO_2 after heat treatment at $650\text{ }^\circ\text{C}$, (c) TiO_2/WO_3 after heat treatment at $650\text{ }^\circ\text{C}$ and (d) $\text{TiO}_2/\text{Na}_2\text{WO}_4 \cdot 2\text{H}_2\text{O}$ after heat treatment at $650\text{ }^\circ\text{C}$

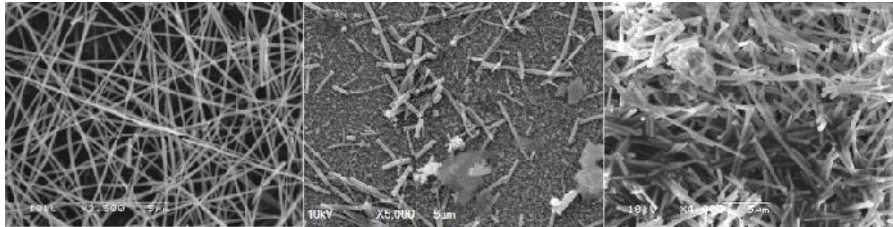


Figure 3. Electron microscopy images of (a) TiO_2 , (b) TiO_2/WO_3 and (c) $\text{TiO}_2/\text{Na}_2\text{WO}_4 \cdot 2\text{H}_2\text{O}$

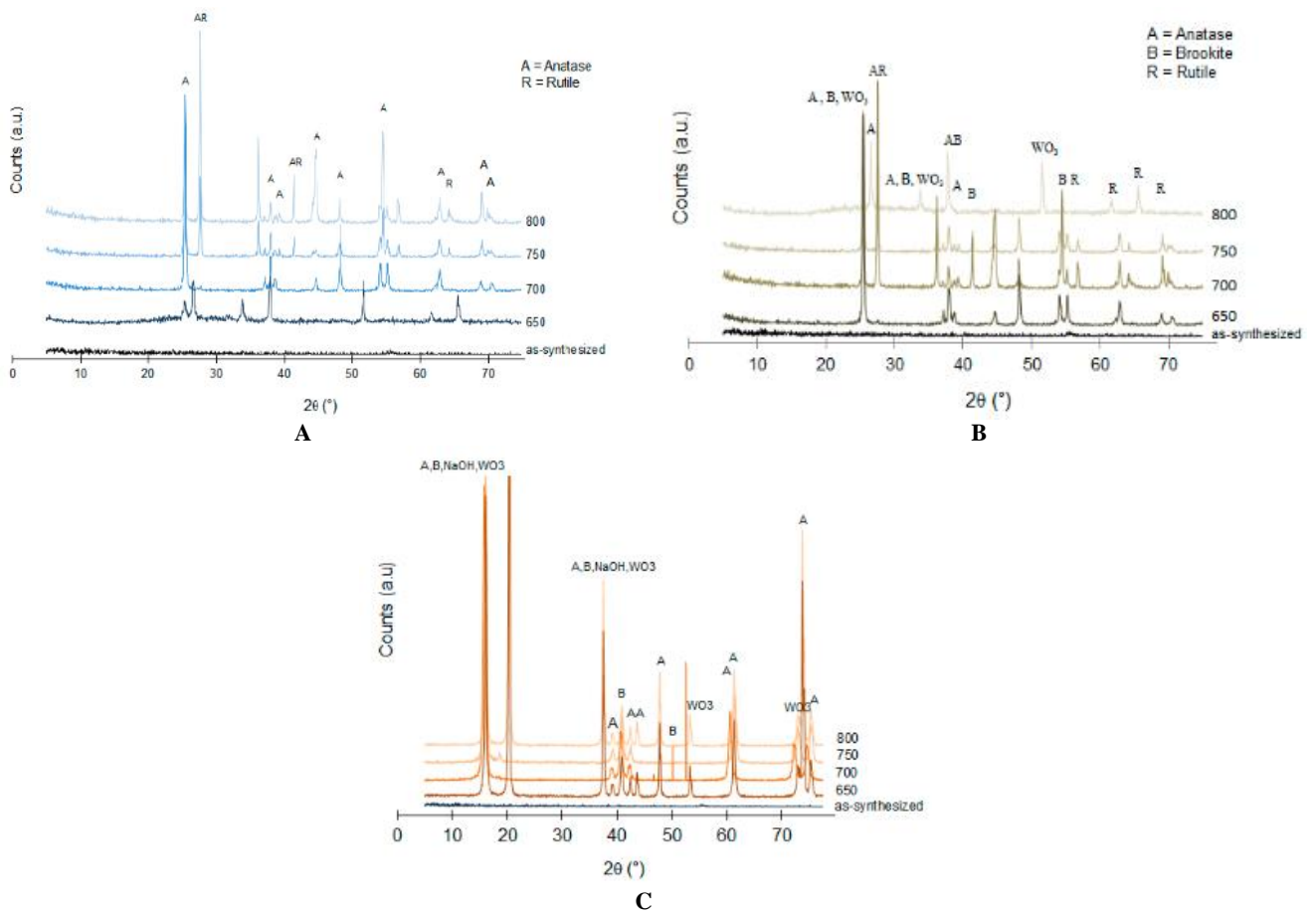


Figure 4. XRD pattern of (a) TiO_2 , (b) TiO_2/WO_3 and (c) $\text{TiO}_2/\text{Na}_2\text{WO}_4 \cdot 2\text{H}_2\text{O}$ films before and after heat-treatment.

Table 1. Colorimetric coordinates that determined the chromogenism in the films

Samples	a*	b*	Hue difference (clear/dark)	L*	Color absorbed
Films TiO ₂ 650 °C	+0.30	- 4.50	-34.14		Blue-Dark
Films TiO ₂ 700 °C	+0.14	-5.25	-53.92		Blue-Dark
Films TiO ₂ 750 °C	+3.15	-1.57	-27.43		Blue-Dark
Films TiO ₂ 800 °C	+3.43	-4.62	-46.04		Blue-Dark
Films TiO ₂ /WO ₃ 650 °C	-1.46	-1.99	68.74		Blue-Clear
Films TiO ₂ /WO ₃ 700 °C	-3.78	-1.59	56.69		Blue-Clear
Films TiO ₂ /WO ₃ 750 °C	-2.97	-1.72	71.64		Blue-Clear
Films TiO ₂ /WO ₃ 800 °C	-1.85	-2.94	54.81		Blue-Clear
Films TiO ₂ /Na ₂ WO ₄ .2H ₂ O 650 °C	+1,41	+4,58	-24.35		Yellow-Orange
Films TiO ₂ /Na ₂ WO ₄ .2H ₂ O 700 °C	+1.37	+3.12	-44.81		Yellow-Orange
Films TiO ₂ /Na ₂ WO ₄ .2H ₂ O 750 °C	+2.55	+1.24	-53.88		Yellow-Orange
Films TiO ₂ /Na ₂ WO ₄ .2H ₂ O 800 °C	+2.16	+5.52	-43.78		Yellow-Orange
Films P25	+ 0.37	-4.46	-32.42		Blue-Dark

Color difference (E *ab)	Classification
0,0 – 0,2	Imperceptible
0,2 – 0,5	Very Little
0,5 – 1,5	Little
1,5 – 3,0	Distinguishable
3,0 – 6,0	Easily Distinguishable
> 6,0	Very Large

Table 3. Chromogenism perceived by human eyes in films

Samples	Color difference (E)	Ability to perceive color chromogen
Films de TiO ₂ 650 °C	2.34	Distinguishable
Films de TiO ₂ 700 °C	2.68	Distinguishable
Films de TiO ₂ 750 °C	2.41	Distinguishable
Films de TiO ₂ 800 °C	2.32	Distinguishable
Films TiO ₂ /WO ₃ 650 °C	3.56	Easily Distinguishable
Films TiO ₂ /WO ₃ 700 °C	3.77	Easily Distinguishable
Films TiO ₂ /WO ₃ 750 °C	3.64	Easily Distinguishable
Films TiO ₂ /WO ₃ 800 °C	3.16	Easily Distinguishable
Films TiO ₂ /Na ₂ WO ₄ .2H ₂ O 650 °C	3.81	Easily Distinguishable
Films TiO ₂ /Na ₂ WO ₄ .2H ₂ O 700 °C	3.44	Easily Distinguishable
Films TiO ₂ /Na ₂ WO ₄ .2H ₂ O 750 °C	3.52	Easily Distinguishable
Films TiO ₂ /Na ₂ WO ₄ .2H ₂ O 800 °C	3.02	Easily Distinguishable
Films P25 (reference)	1,94	Distinguishable

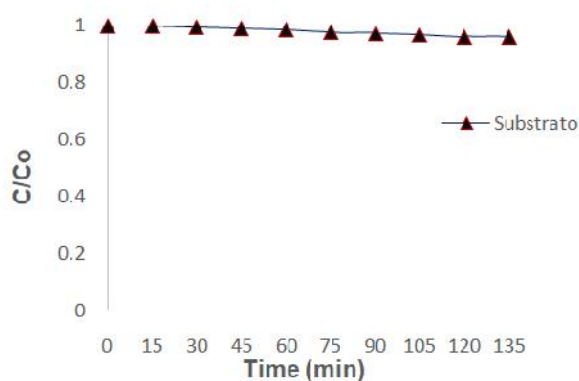


Figure 5. Adsorption test containing only the substrate

This result was already expected, as the TiO₂/WO₃ solution is yellow (Figure 1b), which is the complementary color to blue. Finally, the TiO₂/Na₂WO₄.2H₂O films had maximum light transmittance in the yellow-orange region, influenced by the positive values of a* (red color) and b* (yellow color).

This result was already expected because the TiO₂/Na₂WO₄.2H₂O solution (Figure 1c) is transparent. In the case of a transparent material, all colors not seen in the filter or which do not pass through it are absorbed. Based on this, the color absorbed by the TiO₂/Na₂WO₄.2H₂O films was blue, which is the complementary color to yellow (Soares, 2018). The ability of human eyes to differentiate chromogenic color changes between films was determined by the values obtained by the association of L* (brightness Table 2), E (color difference Table 2) and a (DIN 6174, 1979, Table 2) [Siva, 2007].

The color difference (E) measures the ability of human eyes to differentiate color changes between materials. This visual information was distinguishable for and P25 (reference) TiO₂ films and easily distinguishable for TiO₂/WO₃ and TiO₂/Na₂WO₄.2H₂O films. These results were based on the values of the color difference (E) presented in Table 3. Human eyes cannot distinguish minor color differences (E) that 1.

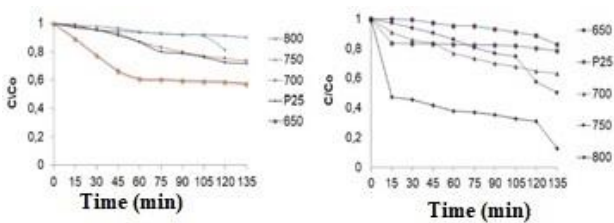


Figure 6. Relative concentration of orange methyl dye in the degradation of TiO_2 and TiO_2/WO_3 films

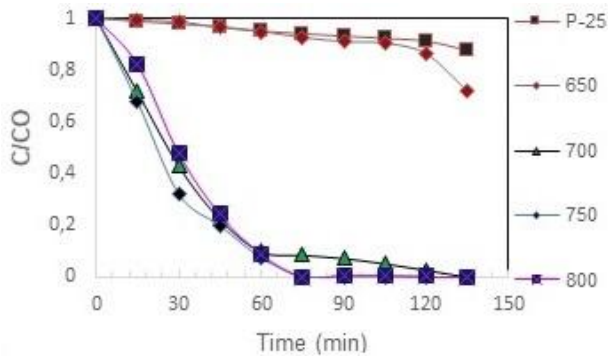


Figure 7. Relative concentration of orange methyl dye in the degradation of $\text{TiO}_2/\text{Na}_2\text{WO}_4 \cdot 2\text{H}_2\text{O}$ films

The Figure 5 shows the adsorption test containing only the substrate submerged in 125 mL of a 20 ppm solution of methyl orange dye, proving through the graph that there are no organic compounds adsorbed on the surface of the substrate. The Figures 6 and 7 show the catalytic activity of the TiO_2 , TiO_2/WO_3 and $\text{TiO}_2/\text{Na}_2\text{WO}_4 \cdot 2\text{H}_2\text{O}$ films, respectively in the degradation of the methyl orange dye, during 135 minutes of exposure to UV-A light ($\lambda = 365 \text{ nm}$). All films could be used as semiconductors in heterogeneous photocatalysis, as all samples were able to degrade the methyl orange dye. The most photoactive TiO_2 films were those that received heat treatment at $650 \text{ }^\circ\text{C}$, managed to degrade approximately 40% of the orange methyl dye in 135 minutes of UVA irradiation. The films treated at $700 \text{ }^\circ\text{C}$ and the P25 standard had a similar behavior, degrading approximately 30% of the dye in 135 minutes of UVA irradiation. And the films treated at $750 \text{ }^\circ\text{C}$ and $800 \text{ }^\circ\text{C}$, degraded approximately 20% and 10%, respectively, of the dye in 135 minutes of UVA irradiation.

This decrease observed in the photoactivity of the films is the result of the formation of the rutile phase, which in this case arises from treatments above $700 \text{ }^\circ\text{C}$. The rutile form is less photoactive than the anatase form and, for this reason, its appearance reduces the photocatalytic activity of the synthesized samples (Feltrin, 2013). The presence of tungsten in the TiO_2/WO_3 films increased the photocatalytic activity of these samples, treated at a temperature of $700 \text{ }^\circ\text{C}$, $750 \text{ }^\circ\text{C}$ and $800 \text{ }^\circ\text{C}$, to approximately 36%, 50% and 90% of degradation, respectively. Such effectiveness is due; the reduction of the band gap from 3.05 eV to 2.89 eV, inhibition of the electron pair/gap recombination $[(e^-)/(h^+)]$, which allowed the transfer of charges between TiO_2 and WO_3 , and the increase in the formation of specific defects (O_2 vacancies). The increase in the temperature of the heat treatment allowed the O_2 vacancies to acquire the mobility necessary to move to a disordered state in the network, increasing the degradation capacity and the efficiency of the process (Muccillo, 2008).

The most effective samples in the degradation of the methyl orange dye were the films containing $\text{TiO}_2/\text{Na}_2\text{WO}_4 \cdot 2\text{H}_2\text{O}$ treated at $700 \text{ }^\circ\text{C}$, $750 \text{ }^\circ\text{C}$ and $800 \text{ }^\circ\text{C}$, respectively. These samples degraded approximately 100% of the dye in 90 minutes of exposure to UV-A radiation. The reasons for the occurrence of such effectiveness are due, in addition to the synergism between the anatase and rutile phases, the reduction of the band gap of the samples, also the presence of sodium associated with the increase in the heat treatment temperature, which increased the number of defects (O_2 vacancies) in the crystalline TiO_2 network. O_2 vacancies are specific defects that occupy atomic network positions and are strongly linked to application in photocatalysis. With the presence of sodium, TiO_2 acquired stability of the structural phase, responsible for increasing the conductivity to the oxygen ion. The increase in the temperature of the heat treatment allowed the O_2 vacancies to acquire the mobility necessary to move to a disordered state in the anionic subnet (Muccillo, 2008). In a study by Chen et. al., describe the obtaining of TiO_2 black nanoparticles with excellent photocatalytic performance, due to the generation of O_2 vacancies.

Conclusion

A The results obtained with the synthesized samples when used in colorimetry and photocatalysis, is due to the synchronicity between the chemical and physical properties of titanium and tungsten oxides, and the occurrence of similar phenomena. In both events, the irradiated light, the band gap energy, the wavelength, and the formation of defects (O_2 vacancies) were essential both for the visual perception of the different colors and for the photoactivity in the degradation of the orange methyl dye. All films could be used as semiconductors in heterogeneous photocatalysis and in colorimetric tests. All samples showed photoactivity in the degradation of the orange methyl dye and chromogenism, that is, they had their color changed during the colorimetry tests. Even the TiO_2 films treated at higher temperatures ($750 \text{ }^\circ\text{C}$ and $800 \text{ }^\circ\text{C}$) that had low photoactivity, showed color changes and the ability to degrade the orange methyl dye. The presence of tungsten and sodium increased the photocatalytic efficiency of the materials, inhibited the recombination of the electron/gap $[(e^-)/(h^+)]$ pair, allowing the transfer of charges between TiO_2 and WO_3 . The increase in the temperature of the heat treatment allowed the O_2 vacancies to acquire the necessary mobility to move to a disordered state in the network, increasing the degradation and light absorption capacity.

Acknowledgment

The authors would like to thank the financial support of the Universidade Federal of Rio Grande do Sul (UFRGS), the Coordenação de Aperfeiçoamento de Pessoal de Nível Superior (CAPES) and Conselho Nacional de Desenvolvimento Científico e Tecnológico (CNPq).

REFERENCES

- Callister, W. D. Jr. 2002. "Ciência e Engenharia de Materiais: Uma introdução", 5ª edição, LTC, Rio de Janeiro, pp.589.
- Chen, S. and Xie, W., 2018. A Facile Approach to Prepare Black TiO_2 with Oxygen Vacancy for Enhancing Photocatalytic Activity, *Nanomaterials*, Vol. 8, pp. 2-16.

- Feltrin, J., Sartor, M.N., De Noni, A. J., Bernardin, A.M., Hotza, D. and Labrincha, J., 2013. Superfícies fotocatalíticas de titânia em substratos cerâmicos. Parte I: Síntese, estrutura e fotoatividade, *Cerâmica*, Vol. 59, pp. 620-632.
- Fioreze, M.E.P.S. and Schmachtenberg, N., 2014. Processos oxidativos avançados: fundamentos e aplicação ambiental, *Revista Eletrônica em Gestão, Educação e Tecnologia Ambiental*, Vol. 18, pp. 9-91.
- Muccillo, E.N.S., 2008. Condutores de íons oxigênio - uma breve revisão, *Cerâmica*, Vol. 54, pp. 129-144.
- Oshani, F., Marandi, R., Rasouli, S. and Farhoud, M.K., 2014. Photocatalytic investigations of TiO₂-P25 nanocomposite thin films prepared by peroxotitanic acid modified sol-gel method, *Applied Surface Science*, Vol. 311, pp. 308-313.
- Silva, R.A., Petter, C.O. and Schneider, I.A.H., 2007. Color loss evaluation of artificially stained agates, *REM: Revista Escola de Minas*, Vol. 60, pp. 477-482.
- Soares, L. and Alves, A., 2018. Photocatalytic properties of TiO₂ and TiO₂/WO₃ films applied as semiconductors in heterogeneous photocatalysis, *Materials Letters*, Vol. 211, pp. 339-342.
- Soares, L. and Alves, A., 2018. Analysis of colorimetry using the CIEL*a*b* system and the photocatalytic activity of photochromic films, *Materials Research Bulletin*, Vol. 105 pp. 318-321.
